Decentralized Direct Adaptive Fuzzy Control for Flexible-Joint Robots

Mohammad Mehdi Fateh, Mahdi Souzanchikashani

Electrical and Robotic Engineering Department, Shahrood University of Technology,
3619995161 Shahrood, Iran.
(Tel: +98273-3393116; e-mail: mmfateh@shahroodut.ac.ir, mahdi_souzanchi@shahroodut.ac.ir)

Abstract: A flexible-joint robot is a complex system with nonlinearity, flexibility and uncertainty. The complexity of conventional methods in modeling and control of robot leads us to apply the fuzzy control. However, stability analysis of the fuzzy control systems is a challenging problem. Based on the guaranteed stability method, this paper presents a novel decentralized direct adaptive fuzzy control approach for the flexible-joint robots. Compared with the majority of control schemes which ignore the actuators, this study considers the whole robotic system including its motors. Instead of the torque control strategy, the proposed approach is based on the voltage control strategy. The common control structure for flexible-joint robots employs two control loops whereas this control design has only one control loop. Compared with the torque-based control approaches, the proposed control is simpler, less computational and more effective. The proposed control design is verified by stability analysis. A comparison with a modified fuzzy proportional-integral controller is presented to show the effectiveness of the proposed fuzzy controller for tracking application.

Keywords: Flexible-joint robot, decentralized control, direct adaptive fuzzy control, voltage control strategy.

1. INTRODUCTION

Control of flexible joint robots has gained an increasing attention due to the complexity of the system characterized by features such as nonlinearity, coupling between the inputs and outputs, joint flexibility, uncertainty and extensive calculations. The torque-based control is the common strategy used for robot manipulators in many control approaches. Various control methods based on the torque control strategy such as PD control (Tomei, 1991), feedback linearization technique (Luca et al., 1985), integral manifold approach (Spong et al., 1987a), singular perturbation method (Marino and Nicosia, 1985), robust control (Spong, 1987b), sliding mode control (Wilson, 1994), adaptive control (Spong, 1985), fuzzy control (Tang et al., 2001), fuzzy adaptive identification and control (Gürkan et al., 2002), learning control (Wang, 1995), neural network control (Zeman et al., 1997), passivity-based impedance control (Kugi et al., 2008), state observer based control (Talole et al., 2010), and adaptive task-space control (Liua et al., 2008) have been proposed for flexible joint robots.

The torque control strategy is based on a fact that the motion of robot is caused by the joint torques, thereby the joint torques are given as the control commands. However, the torque-based control approaches will become complex to overcome the dynamical features mentioned above. Furthermore, it is assumed that the actuators can perfectly provide the torque commands. Then, the actuator dynamics are ignored while they become important in performing high-speed and precise tasks. To remove these shortcomings, voltage control strategy was proposed (Fateh, 2008). This strategy considers the voltages of motors as the inputs of the robotic system including the actuators and robot manipulator. A voltage control scheme can be free from manipulator dynamics, thus will make the control problem simple. Some control schemes based on the voltage control strategy such as robust time-delay control (Fateh, 2012a) and nonlinear adaptive control (Fateh, 2012b) have been devoted to deal with flexible-joint robot manipulators.

The conventional control methods proposed for flexible joint robots have mentioned the flexibility as a challenging problem. Flexibility in joints occurs due to the deformation of transmission systems such as harmonic gears (Sweet and Good, 1985). Compared with rigid robots, number of degrees of freedom becomes twice the number of control actions because of flexibility in the joints, and the matching property between nonlinearities and inputs is lost (Brogliato et al., 1995). As a result, the link position cannot directly follow the actuator position. The controllers should compensate the flexibility in joints for improving the performance, avoiding unwanted oscillations, and establishing the stability.

Fuzzy control is a good alternative, for the control of nonlinear uncertain systems. A large class of nonlinear systems can be well approximated by Takagi-Sugeno fuzzy models (Lendek et al., 2010). The most successful implementations of the fuzzy control are where the process under control is too complex for analysis and control by conventional methods (Homaifar et al., 1994). It becomes superior to conventional control due to using information from experts in linguistic rules (Wang, 1996). Moreover, a

fuzzy system can be used as a universal approximator for any nonlinear function. This feature has been efficiently used to design many fuzzy controllers such as adaptive fuzzy controllers. The direct method of Lyapunov has been successfully used in the design and analysis of adaptive fuzzy control. Wang is a pioneer to propose such a controller (Wang, 1996). This controller can be applied for companion form systems with constant control gain with no external disturbances. Based on the Lyapanov stability method, a multi-input/multi-output adaptive fuzzy terminal sliding-mode controller for robotic manipulators was designed (Li and Huang, 2010). Robust stabilization for nonlinear systems was developed based on a switched fuzzy control law (Jabri et al., 2012). Adaptive fuzzy control has been well used for large-scale systems (Tong et al., 2004), single-input/single-output systems (Tong et al., 2004), stochastic strict-feedback systems (Li et al., 2010), and multi-input/multi-output systems (Hsua and Fua, 2006). The design of adaptive fuzzy control in decentralized structure with guaranteed stability, robustness, satisfactory performance and ease of implementation is now the main concern of the researchers.

The decentralized controller has been used by majority of industrial robots in favour of computational simplicity and ease of implementation (Seraji, 1989). In the decentralized control, an actuator is commanded to drive a joint by taking feedbacks from that joint (Liua et al., 2008). Therefore, the voltage control strategy can be well fitted for providing the decentralized control. For this purpose, the decentralized control must be capable to overcome the effects of decentralizing the robotic system. These effects are twofold. First, the robotic system is multivariable with coupling between the inputs and outputs. Second, the degrees of freedom are twice the number of control inputs because of flexibility in the joints. Therefore, decomposing a robotic system to individual single-input/single-output systems for applying the decentralized control is a challenging problem which degrades the performance of decentralized control. In this paper, the decentralized control is well performed by the ability of fuzzy system to overcome uncertainty which contains the effects of decentralizing the robotic system.

To overcome the mentioned problems, a decentralized Direct Adaptive Fuzzy Control (DAFC) is developed based on the guaranteed stability. Unlike the presented control schemes for the flexible joint robots, the proposed control does not follow the torque control strategy. In contrast, it is based on the voltage control strategy which is simpler, less computational and more effective than the torque control strategy. Instead of using two control loops as used in the majority of previous controllers, it directly controls the joint position via one control loop. The position error, its derivative and its integral are used as feedbacks whereas the controller has a simple structure using only nine fuzzy rules. The effectiveness of the control design is shown though a comparison with a Modified Fuzzy Proportional-Integral Controller (MFPIC) (Tang et al., 2001).

The paper is organized as follows: Section 2 presents the modelling of flexible-joint robot. Section 3 develops the decentralized DAFC and presents the stability analysis. Section 4 provides the simulation results and a comparison with the MFPIC. Finally, Section 5 concludes the paper.

2. MODELLING

Consider a flexible-joint robot which is driven by geared permanent magnet dc motors. If the joint flexibility is modeled by a linear torsional spring, dynamic equation of motion can be expressed as

$$\mathbf{D(q)\ddot{q}+C(q,\dot{q})\dot{q}+g(q)=K(r\theta_m-q)} \quad (1)$$

$$\mathbf{J\ddot{\theta}_m+B\dot{\theta}_m+rK(r\theta_m-q)=\tau_m} \quad (2)$$

where $\mathbf{q}\in R^n$ is a vector of joint angles and $\boldsymbol{\theta}_\mathbf{m}\in R^n$ is a vector of rotor angles. Thus, this system possesses $2n$ coordinates as $[\mathbf{q}\ \ \boldsymbol{\theta}_\mathbf{m}]$. $\mathbf{D(q)}$ is a $n\times n$ matrix of manipulator inertia, $\mathbf{C(q,\dot{q})\dot{q}}\in R^n$ is a vector of centrifugal and Coriolis forces, $\mathbf{g(q)}\in R^n$ is a vector of gravitational forces and $\boldsymbol{\tau}_{\boldsymbol{m}}\in R^n$ is a torque vector of motors. $\mathbf{J}$, $\mathbf{B}$ and $\mathbf{r}$ are $n\times n$ diagonal matrices to represent coefficients of the motor inertia, motor damping and reduction gear, respectively. The diagonal matrix $\mathbf{K}$ represents the lumped flexibility of the joint and reduction gear together. To simplify the model, both the joint stiffness and gear coefficients are assumed constant. The vector of gravitational forces $\mathbf{g(q)}$ is assumed function of only the joint positions as used in a simplified model given by (Hsua and Fua, 2006). Note that vectors and matrices are bold for clarity.

System (1)-(2) is highly nonlinear, computationally extensive, heavily coupled, multi-input/multi-output system with the $2n$ coordinates. Complexity of model has been a serious challenge in the robot modeling and control as shown by literature. It is expected to face higher complexity if the proposed model includes the actuator dynamics.

Consider the geared permanent magnet dc motors which drives the robot manipulator. The voltage equation in the matrix form is expressed as

$$\mathbf{RI_a+L\dot{I}_a+K_b\dot{\theta}_m+\varphi=v} \quad (3)$$

where $\mathbf{v}\in R^n$ is a vector of motor voltages, $\mathbf{I_a}\in R^n$ is a vector of motor currents and $\dot{\boldsymbol{\theta}}_\mathbf{m}\in R^n$ is a vector of rotor velocities. $\mathbf{R}$, $\mathbf{L}$ and $\mathbf{K_b}$ represent the $n\times n$ diagonal matrices for the coefficients of armature resistance, armature inductance, and back-emf constant, respectively. $\boldsymbol{\varphi}\in R^n$ is a vector of external disturbances.

The motor torques $\boldsymbol{\tau}_\mathbf{m}$ as input for dynamic equation (2) is produced by the motor currents as

$$\mathbf{K_mI_a}=\boldsymbol{\tau}_\mathbf{m} \quad (4)$$

where $\mathbf{K_m}$ is a diagonal matrix of the torque constants. Equations (1)-(4) forms the robotic system such that the voltage vector $\mathbf{v}$ is the input vector and the joint angle vector

$\mathbf{q}$ is the output vector. Using (1)-(4), the state space model of the robotic system can be derived as

$$\dot{\mathbf{x}} = \mathbf{f}(\mathbf{x}) + \mathbf{b}(\mathbf{v} - \boldsymbol{\varphi}) \tag{5}$$

where

$$\mathbf{f}(\mathbf{x}) = \begin{bmatrix} \mathbf{x}_2 \\ \mathbf{D}^{-1}(\mathbf{x}_1)\left(-\mathbf{g}(\mathbf{x}_1) - \mathbf{K}\mathbf{x}_1 - \mathbf{C}(\mathbf{x}_1, \mathbf{x}_2)\mathbf{x}_2 + \mathbf{K}\mathbf{r}\mathbf{x}_3\right) \\ \mathbf{x}_4 \\ \mathbf{J}^{-1}\left(\mathbf{r}\mathbf{K}\mathbf{x}_1 - \mathbf{r}^2\mathbf{K}\mathbf{x}_3 - \mathbf{B}\mathbf{x}_4 + \mathbf{K}_m\mathbf{x}_5\right) \\ -\mathbf{L}^{-1}\left(\mathbf{K}_b\mathbf{x}_4 + \mathbf{R}\mathbf{x}_5\right) \end{bmatrix}$$

$$\mathbf{b} = \begin{bmatrix} \mathbf{0} \\ \mathbf{0} \\ \mathbf{0} \\ \mathbf{0} \\ \mathbf{L}^{-1} \end{bmatrix}, \quad \mathbf{x} = \begin{bmatrix} \mathbf{q} \\ \dot{\mathbf{q}} \\ \boldsymbol{\theta}_m \\ \dot{\boldsymbol{\theta}}_m \\ \mathbf{I}_a \end{bmatrix} \tag{6}$$

The state space model of the robotic system expressed by (5) shows a highly nonlinear coupled large system with the state vector of $\mathbf{x}$ in the dimension of $5n \times 1$. In addition, the state space model is not in companion form. By extensive calculations, a companion form can be obtained. However, such a complex model is not useful from a control point of view due to the computational burden.

3. DAFC DESIGN

In order to design a decentralized controller, a decoupled model of the robotic system is introduced. Let us define

$$\mathbf{r}\boldsymbol{\theta}_m - \mathbf{q} = \boldsymbol{\delta} \tag{7}$$

where $\boldsymbol{\delta}$ shows the effect of joint flexibility. A rigid robot which has no flexibility in the joints with $\mathbf{r}\boldsymbol{\theta}_m = \mathbf{q}$ provides that $\boldsymbol{\delta} = 0$. Substituting (7) into (2) yields

$$\mathbf{J}\ddot{\boldsymbol{\theta}}_m + \mathbf{B}\dot{\boldsymbol{\theta}}_m + \mathbf{r}\mathbf{K}\boldsymbol{\delta} = \boldsymbol{\tau}_m \tag{8}$$

Using (3), (4), (7) and (8), a decoupled equation can be formed as

$$\ddot{\mathbf{q}} + \mathbf{K}_a\dot{\mathbf{q}} + \boldsymbol{\mu} = \mathbf{K}_v\mathbf{v} \tag{9}$$

where $\mathbf{K}_a$ and $\mathbf{K}_v$ are diagonal matrices and $\boldsymbol{\mu}$ is a vector of lamped uncertainty expressed by

$$\mathbf{K}_a = \mathbf{J}^{-1}\left(\mathbf{B} + \mathbf{K}_m\mathbf{R}^{-1}\mathbf{K}_b\right) \tag{10}$$

$$\mathbf{K}_v = \mathbf{r}\mathbf{J}^{-1}\mathbf{K}_m\mathbf{R}^{-1} \tag{11}$$

$$\boldsymbol{\mu} = \mathbf{r}\ddot{\boldsymbol{\delta}} + \mathbf{r}\mathbf{K}_a\dot{\boldsymbol{\delta}} + \mathbf{J}^{-1}\mathbf{r}^2\mathbf{K}\boldsymbol{\delta} + \mathbf{K}_v\left(\mathbf{L}\dot{\mathbf{I}}_a + \boldsymbol{\varphi}\right) \tag{12}$$

According to (9), the dynamics of the *ith* joint in the scalar form is represented as

$$\ddot{q} + K_a\dot{q} + \mu = K_v v \tag{13}$$

where the presented variables $\ddot{q}$, $\dot{q}$, μ and v are the *ith* element of the vectors $\ddot{\mathbf{q}}$, $\dot{\mathbf{q}}$, $\boldsymbol{\mu}$ and $\mathbf{v}$, respectively. The coefficients K_a and K_v are the *ith* element of the diagonal of matrices $\mathbf{K}_a$ and $\mathbf{K}_v$, respectively.

3.1 Proposed Design

We design a decentralized fuzzy controller by the use of two variables as inputs to the fuzzy controller namely x_1 and x_2 defined as

$$x_1 = e + k_1\int e \tag{14}$$

$$x_2 = \dot{e} + k_1 e \tag{15}$$

where e is the tracking error expressed by

$$e = q_d - q \tag{16}$$

in which q_d and q, are the desired and actual joint positions, respectively. The motor voltage, v, is the output of the controller.

If three membership functions are given to each fuzzy input, the whole control space is covered by nine fuzzy rules. The linguistic fuzzy rules are proposed in the form of Mamdani type as

$$Rule\ l: \text{If } x_1 \text{ is } A_l \text{ and } x_2 \text{ is } B_l \text{ Then } v \text{ is } C_l \tag{17}$$

where *Rule l* denotes the *l*th fuzzy rule for $l = 1,...,9$. In the *l*th rule, A_l, B_l and C_l are fuzzy membership functions belonging to the fuzzy variables x_1, x_2 and v, respectively. Using the membership functions and fuzzy rules, we design the fuzzy controller. In a good design, the set of rules should be complete, consistent, and continuous (Wang, 1996). It is complete if at any point in the input space there is at least one rule that the membership value of the IF part of the rule at this point is non-zero. It is consistent if there are no rules with the same IF parts but different THEN parts. It is continuous if THEN parts of the neighboring rules have intersection. In order to design a membership function, we select the centre, range, and shape of the membership function. The operating range of input variables should be covered by membership functions. To cover a large range, the membership function located in the left and right sides can be selected as sigmoid function whereas the membership function in the centre can be Gaussian function. Therefore, three membership functions named as P, Z and N are given to the input x_1 in the operating range of manipulator. They are expressed as

$$\mu_P(x_1) = \begin{cases} 0 & x_1 \le 0 \\ 2x_1^2 & 0 \le x_1 \le 0.5 \\ 1 - 2(x_1 - 1)^2 & 0.5 \le x_1 \le 1 \\ 1 & x_1 \ge 1 \end{cases},$$

$$\mu_N(x_1) = \begin{cases} 1 & x_1 \le -1 \\ 1 - 2(x_1 + 1)^2 & -1 \le x_1 \le -0.5 \\ 2x_1^2 & -0.5 \le x_1 \le 0 \\ 0 & x_1 \ge 0 \end{cases}$$

$$\mu_Z(x_1) = \exp\left(-x_1^2 / (2\sigma^2)\right), \quad \sigma = 0.3 \tag{18}$$

The membership function $\mu_P(x_1)$ corresponds to positive values of x_1, the membership function $\mu_N(x_1)$ corresponds to negative values of x_1, and the membership function $\mu_Z(x_1)$ corresponds to about zero values of x_1. The membership functions belonging to x_2 are given the same as x_1. The membership functions of output v in the Gaussian shapes are expressed by

$$\mu_{C_l}(v) = \exp\left(-\left((v-\hat{y}_l)^2/(2\sigma^2)\right)\right) \tag{19}$$

where $\hat{y}_l$ is the center of C_l.

Using (17)–(19), the fuzzy rule base is formed. If we use the Mamdani type inference engine, the singleton fuzzifier and the center average defuzzifier (Wang, 1996), v is calculated as

$$v = \sum_{l=1}^{9} \hat{y}_l \psi_l(x_1,x_2) = \hat{\mathbf{y}}^{\mathrm{T}} \boldsymbol{\psi}(x_1,x_2) \tag{20}$$

where $\boldsymbol{\psi} = \begin{bmatrix}\psi_1 & \dots & \psi_9\end{bmatrix}^T$ in which ψ_l is a positive value expressed as

$$\psi_l(x_1,x_2) = \frac{\mu_{A_l}(x_1)\mu_{B_l}(x_2)}{\sum_{l=1}^{9}\mu_{A_l}(x_1)\mu_{B_l}(x_2)} \tag{21}$$

where $\mu_{A_l}, \mu_{B_l} \in [0,1]$. The parameters $\hat{\mathbf{y}}$ in (20) are determined by adaptive rule afterward. An important contribution of fuzzy systems theory is to provide a systematic procedure for transforming a set of linguistic rules into a nonlinear mapping given by (20).

Applying fuzzy controller (20) to system (14) obtains the closed-loop system

$$\ddot{q} + K_a\dot{q} + \mu = K_v\hat{\mathbf{y}}^T\boldsymbol{\psi}(x_1,x_2) \tag{22}$$

where $\hat{\mathbf{y}}$ is the estimation of $\mathbf{y}$ used into a fuzzy system $\mathbf{y}^T\boldsymbol{\psi}(e,\dot{e})$ which approximates the following function based on the universal approximation theorem of fuzzy systems as

$$K_v^{-1}\left(\ddot{q}_d + k_1\dot{e} + k_d x_2 + k_p x_1 + K_a\dot{q} + \mu\right) = \mathbf{y}^T\boldsymbol{\psi}(x_1,x_2) + \varepsilon \tag{23}$$

where ε is the approximation error, k_p, k_d and k_1 are positive gains which are selected as a control design parameters.

In order to obtain the adaptive law, we form the tracking system from (22) and (23) as

$$\dot{x}_2 + k_d x_2 + k_p x_1 = k_v\left(\mathbf{y}-\hat{\mathbf{y}}\right)^T\boldsymbol{\psi}(x_1,x_2) + k_v\varepsilon \tag{24}$$

The state space equation in the tracking space is obtained using (24) as

$$\dot{\mathbf{X}} = \mathbf{A}\mathbf{X} + \mathbf{B}w \tag{25}$$

Where

$$\mathbf{A} = \begin{bmatrix}0 & 1\\ -k_p & -k_d\end{bmatrix}, \quad \mathbf{B} = \begin{bmatrix}0\\1\end{bmatrix}, \quad \mathbf{X} = \begin{bmatrix}x_1\\x_2\end{bmatrix},$$

$$w = k_v\left(\mathbf{y}-\hat{\mathbf{y}}\right)^T\boldsymbol{\psi} + k_v\varepsilon \tag{26}$$

A positive definite function F is suggested as

$$F = 0.5\mathbf{X}^T\mathbf{P}\mathbf{X} + \frac{k_v}{2\alpha}\left(\mathbf{y}^T-\hat{\mathbf{y}}^T\right)\left(\mathbf{y}-\hat{\mathbf{y}}\right) \tag{27}$$

where the constant $\alpha > 0$, $\mathbf{P}$ and $\mathbf{Q}$ are the unique symmetric, positive definite matrices satisfying the matrix Lyapunov equation

$$\mathbf{A}^T\mathbf{P} + \mathbf{P}\mathbf{A} = -\mathbf{Q} \tag{28}$$

Then, $\dot{F}$ is calculated using (25)-(28) as

$$\dot{F} = -0.5\mathbf{X}^T\mathbf{Q}\mathbf{X} + \mathbf{X}^T\mathbf{P}_2k_v\left(\left(\mathbf{y}^T-\hat{\mathbf{y}}^T\right)\boldsymbol{\psi}+\varepsilon\right) - \frac{k_v}{\alpha}\left(\mathbf{y}^T-\hat{\mathbf{y}}^T\right)\dot{\hat{\mathbf{y}}} \tag{29}$$

where $\mathbf{P}_2$ is the second column of $\mathbf{P}$. Note that $\mathbf{X}^T\mathbf{P}_2$, thus (29) can be represeted as

$$\dot{F} = -0.5\mathbf{X}^T\mathbf{Q}\mathbf{X} + k_v\left(\mathbf{y}^T-\hat{\mathbf{y}}^T\right)\left(\mathbf{X}^T\mathbf{P}_2\boldsymbol{\psi} - \frac{1}{\alpha}\dot{\hat{\mathbf{y}}}\right) + \mathbf{X}^T\mathbf{P}_2k_v\varepsilon \tag{30}$$

If the adaptive law is given by

$$\dot{\hat{\mathbf{y}}} = \alpha\mathbf{X}^T\mathbf{P}_2\boldsymbol{\psi} \tag{31}$$

we have

$$\dot{F} = -0.5\mathbf{X}^T\mathbf{Q}\mathbf{X} + \mathbf{X}^T\mathbf{P}_2k_v\varepsilon \tag{32}$$

The tracking error reduces if $\dot{F} < 0$. Thus, satisfying $\dot{F} < 0$ results in

$$\mathbf{X}^T\mathbf{P}_2k_v\varepsilon < 0.5\mathbf{X}^T\mathbf{Q}\mathbf{X} \tag{33}$$

One can imply $\lambda_{\min}(\mathbf{Q})\|\mathbf{X}\|^2 \le \mathbf{X}^T\mathbf{Q}\mathbf{X} \le \lambda_{\max}(\mathbf{Q})\|\mathbf{X}\|^2$ where $\lambda_{\min}(\mathbf{Q})$ and $\lambda_{\max}(\mathbf{Q})$ are the minimum and maximum eigenvalues of $\mathbf{Q}$, respectively. To satisfy $\dot{F} < 0$ it is sufficient that

$$2k_v\|\mathbf{P}_2\|.|\varepsilon| / \lambda_{\min}(\mathbf{Q}) < \|\mathbf{X}\| \tag{34}$$

The tracking error becomes small in the area defined by (34). As a result, the tracking error ultimately enters into the ball with the radius of $2k_v\|\mathbf{P}_2\|.|\varepsilon| / \lambda_{\min}(\mathbf{Q})$.

A block diagram of the proposed design is shown in Fig. 1. In general, the proposed adaptive controller can be applied to every joint of a robotic system known as the electrically driven robot manipulator. The adaptive law (31) will adapt the controller to be effective in tracking the desired trajectory for every joint. In fact, the adaptive law (31) regulates, $\hat{\mathbf{y}}$, the centres of membership functions for output v as

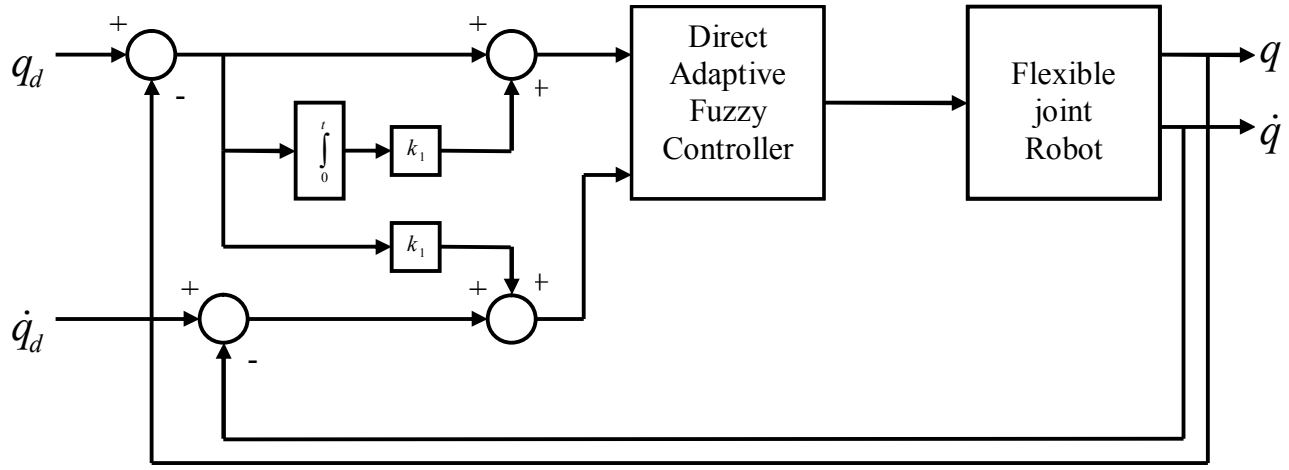

Fig. 1. The block diagram of the DAFC.

$$\hat{\mathbf{y}} = \int_0^t \alpha \mathbf{X}^T \mathbf{P}_2 \boldsymbol{\psi} dt + \hat{\mathbf{y}}(0) \tag{35}$$

where $\hat{\mathbf{y}}(0)$ is the initial value of $\hat{\mathbf{y}}$ that can be given zero. Considering $\boldsymbol{\psi}(x_1, x_2)$ and $\mathbf{X} = \begin{bmatrix} x_1 & x_2 \end{bmatrix}^T$, we need feedbacks of x_1 and x_2 to compute $\hat{\mathbf{y}}$.

3.2 Stability Analysis

In order to guarantee the stability and provide a robust tracking performance of the proposed controller in the presence of uncertainty, some assumptions are required.

To make the dynamics of tracking error well defined such that the robot can track the desired trajectory the following assumption is made.

Assumption 1: The desired trajectory q_d must be smooth in the sense that q_d and its derivatives up to a necessary order are available and all uniformly bounded (Liua et al., 2008).

As a necessary condition to design a robust control, the external disturbance must be bounded as given in *Assumption 2*.

Assumption 2: The external disturbance $\varphi(t)$ is bounded as

$|\varphi(t)| \le \varphi_{\max}$, where $\varphi_{\max}$ is a positive constant.

The electric motor should be protected against the over-voltage. Thus, we make the next assumption:

Assumption 3: The motor voltage is bounded as

$$|v| \le v_{\max} \tag{36}$$

The motor should be sufficiently strong to follow the desired joint velocity under the maximum permitted voltages. Therefore, the following assumption is made.

Assumption 4: Assume that

$$\left| RI_a + L\dot{I}_a + k_b\dot{\theta}_m + \varphi(t) \right| \le \rho(t) < u_{\max} \tag{37}$$

where $\rho(t)$ is a positive scalar.

Based on the reasoning in Section 3, $\dot{F} < 0$ implies that $2k_v \|\mathbf{P}_2\| . |\varepsilon| / \lambda_{\min}(\mathbf{Q}) < \|\mathbf{X}\|$ in (34) and $\|\mathbf{X}\| \le \|\mathbf{X}(0)\|$ where $\mathbf{X}(0)$ is the initial values of $\mathbf{X}$. Hence,

$$2k_v \|\mathbf{P}_2\| . |\varepsilon| / \lambda_{\min}(\mathbf{Q}) < \|\mathbf{X}\| \le \|\mathbf{X}(0)\| \tag{38}$$

Therefore, $\mathbf{X}$ is bounded where $\mathbf{X}$ is expressed as $\mathbf{X}^T = \begin{bmatrix} x_1 & x_2 \end{bmatrix}$, $x_1 = e + k_1 \int e$ and $x_2 = \dot{e} + k_1 e$ as expressed by (14) and (15). The linear equation $\dot{e} + k_1 e = x_2$ has the bounded input x_2, thereby e and $\dot{e}$ are bounded.

Extending this result to all motors obtains the boundedness of e and $\dot{e}$ for all joints.

The desired trajectory q_d and its derivative $\dot{q}_d$ are assumed bounded in *Assumption 1*. Since $e = q_d - q$ and $\dot{e} = \dot{q}_d - \dot{q}$, thus boundedness of e and $\dot{e}$ follows boundedness of q and $\dot{q}$. Appling the same analysis to all motors implies the boundedness of system states $\mathbf{q}$ and $\dot{\mathbf{q}}$.

Assumption 3 obtains that $\hat{\mathbf{y}}^{\mathbf{T}} \boldsymbol{\psi} \le u_{\max}$ while $\boldsymbol{\psi}$ is bounded, thus the estimate parameters $\hat{\mathbf{y}}$ are bounded.

Inequality (38) implies the boundedness of approximation error ε.

Assumption 3 implies that the motor voltage u is bounded, thus according to a proof given by (Tong et al., 2004) I_a and $\dot{\theta}_m$ are bounded. Appling the same analysis to all motors implies the boundedness of system states $\mathbf{I_a}$ and $\dot{\boldsymbol{\theta}}_{\mathbf{m}}$.

As proven above, the state vectors $\mathbf{q}, \dot{\mathbf{q}}$, $\mathbf{I_a}$ and $\dot{\boldsymbol{\theta}}_\mathbf{m}$ are bounded. The boundedness of $\boldsymbol{\theta}_\mathbf{m}$ is proven as follows: substituting (4) into (2) yields

$$\mathbf{J}\ddot{\boldsymbol{\theta}}_\mathbf{m} + \mathbf{B}\dot{\boldsymbol{\theta}}_\mathbf{m} + \mathbf{r}^2\mathbf{K}\boldsymbol{\theta}_\mathbf{m} = \mathbf{K}_\mathbf{m}\mathbf{I}_\mathbf{a} + \mathbf{rKq} \tag{39}$$

Since $\mathbf{J}$, $\mathbf{B}$ and $\mathbf{r}^2\mathbf{K}$ are positive diagonal matrices, the linear system expressed by (39) is stable with the bounded input $\mathbf{K}_\mathbf{m}\mathbf{I}_\mathbf{a} + \mathbf{rKq}$. As a result, the output $\boldsymbol{\theta}_\mathbf{m}$ is bounded. In summary all system states defined in (6) are bounded. It is thus concluded that the proposed DAFC has a guaranteed stability.

4. SIMULATION

The DAFC is simulated on a SCARA robot driven by permanent magnet dc motors as shown in Fig. 2. The four controllers are given the same for the sake of simplicity. The Denavit–Hartenberg (DH) parameters of the SCARA robot are given in Table 1, where the parameter θ_i, d_i, a_i and α_i are called the joint angle, link offset, link length, and link twist, respectively. The dynamical parameters of the manipulator are given in Table 2, that is, for the i th link, m_i is the mass, $r_{ci} = [x_{ci} \quad y_{ci} \quad z_{ci}]^T$ is the center of mass expressed in the i th frame, and I_i is the inertia tensor expressed in the center of mass frame defined as

$$I_i = \begin{bmatrix} I_{xxi} & I_{xyi} & I_{xzi} \\ I_{xyi} & I_{yyi} & I_{yzi} \\ I_{xzi} & I_{yzi} & I_{zzi} \end{bmatrix} \tag{40}$$

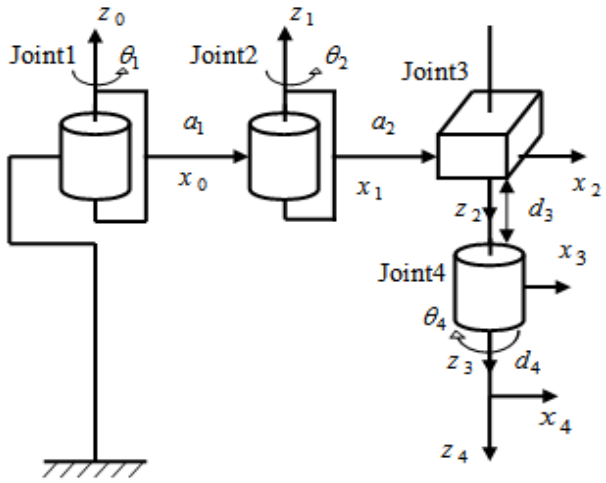

Fig. 2. Symbolic representation of the SCARA robot.

The parameters of motors are given in Table 3. The desired position for joint 1, 2 and 4 is given by

$$q_d = (\pi/150)t^2 - (\pi/3375)t^3 \tag{41}$$

And the desired position for joint 3 is given by

$$q_d = (\pi/750)t^2 - (\pi/16875)t^3 \tag{42}$$

The desired joint trajectories are shown in Fig. 3 and Fig. 4. The desired trajectory should be sufficiently smooth such that all its derivatives up to the required order are bounded.

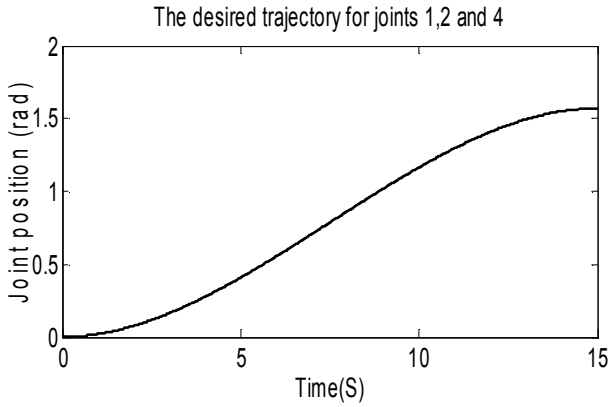

Fig. 3. The desired trajectories for joints 1, 2 and 4.

Table 1. The D-H parameters.

i	$\theta\ (rad)$	$d\ (m)$	$a\ (m)$	$\alpha\ (rad)$
1	θ_1	0	$a_1 = 0.6$	0
2	θ_2	0	$a_2 = 0.4$	π
3	0	d_3	0	0
4	θ_4	$d_4 = 0.08$	0	0

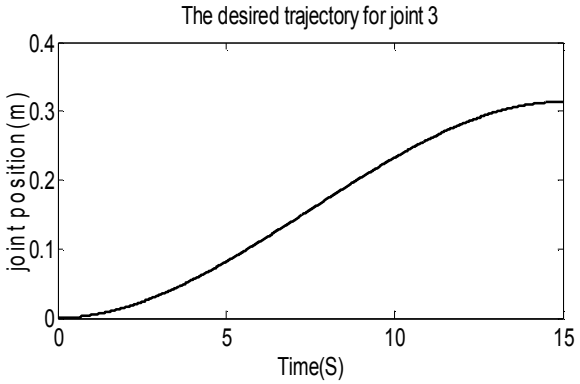

Fig. 4. The desired trajectory for joint 3.

Simulation 1: The DAFC is simulated. All controllers have the same design parameters $k_p = 1$, $k_d = 1$, and $k_1 = 0.4$. The gain α for the adapting the controllers 1, 2, 3 and 4 is set to 200, 600, 500 and 400, respectively. The performance of the control system is satisfactory in the operating time of the desired trajectories for $15\,S$ as shown in Fig. 5. The maximum values of tracking errors for the joints 1, 2, 3, and 4 are $0.049rad$, $-0.069rad$, $0.007m$ and $0.005rad$, respectively. The effects of the flexibility in joints appeared in the first part of responses are reduced well. Among the joints, joint 1 is affected further than other since such dynamical effects are transferred to joint 1 in a serial chain such as the robot. The control efforts behave well under the maximum voltages without the chattering problem as shown in Fig. 6. The currents of motors are shown in Fig. 7 in which the maximum values for the motors 1, 2, 3 and 4 are $0.61A$,

$0.53A$, $-3.7A$ and $0.003A$, respectively. Motor 3 actually has the maximum load. The adapting parameters $\hat{y}$ are shown in Fig. 8. It is noted that all nine adapting parameters for each controller are the same such that we cannot recognize them from each other.

Table 2. The dynamical parameters of SCARA robot.

i	x_i (m)	y_i (m)	z_i (m)	m_i (kg)	I_{xxi} (kgm^2)	I_{yyi} (kgm^2)	I_{zzi} (kgm^2)	I_{xyi} (kgm^2)	I_{xzi} (kgm^2)	I_{yzi} (kgm^2)
1	-0.318	0	0	26.14	0.0939	1.3441	1.3996	0	0.0051	0
2	-0.274	0	0	19.1	0.1947	0.6156	0.5144	0.0001	-0.0187	0.0001
3	0	0	-0.298	2.35	0.0695	0.0695	0.0002	0	0	0
4	0	0	-0.039	0.38	0.0002	0.0002	4.3×10^{-5}	0	0	0

Table 3. The parameters of the dc motors.

$\mathbf{u_{max}}$ (V)	**R** (Ω)	$\mathbf{K_b}$ $\left(\frac{V\,s}{rad}\right)$	**L** (H)	$\mathbf{J_m}$ $\left(\frac{Nm\,s^2}{rad}\right)$	$\mathbf{B_m}$ $\left(\frac{Nm\,s}{rad}\right)$	**r**	**K** $\left(\frac{Nm}{rad}\right)$
42	1.6	0.26	0.001	0.0002	0.001	0.01	750

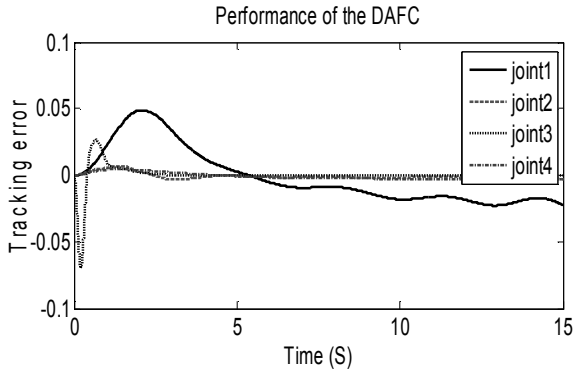

Fig. 5. The performance of the DAFC.

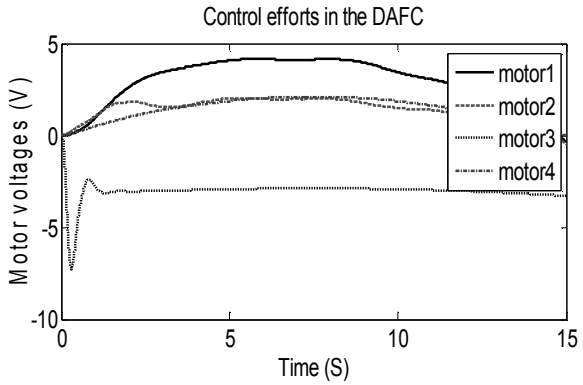

Fig. 6. Control efforts of the DAFC.

Simulation 2: The modified fuzzy PI control MFPIC given by (Tang et al., 2001) is simulated and compared with the DAFC. The controller is a fuzzy PI controller with an automatic gain output as expressed through a block diagram in Fig. 9. The controller requires feedbacks of the joint position and velocity, motor position and torque. The fuzzy controller has two inputs namely the tracking error and its derivative. The controller is formed by using three membership functions for each input plus six fuzzy logic rules. In order to have a fair comparison, the control algorithms are simulated on the SCARA robot. The sampling period is given $T = 0.001S$ and the parameters of controllers are given in Table 4.

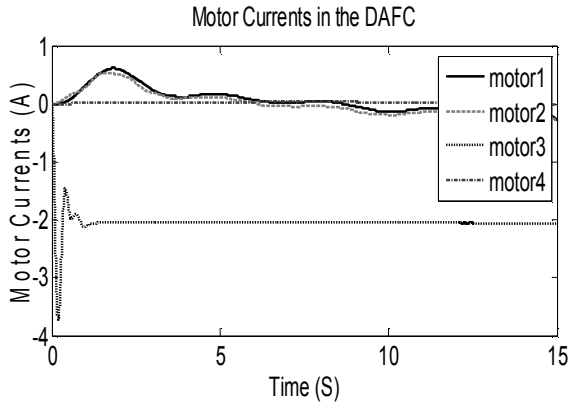

Fig. 7. Motor currents in the DAFC.

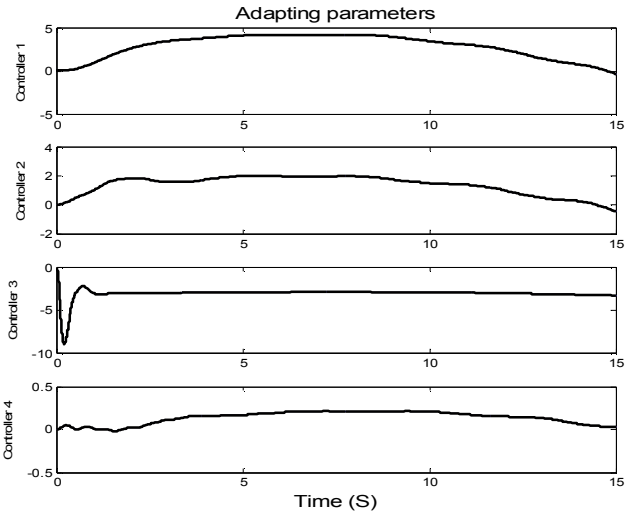

Fig. 8. Adapting parameters.

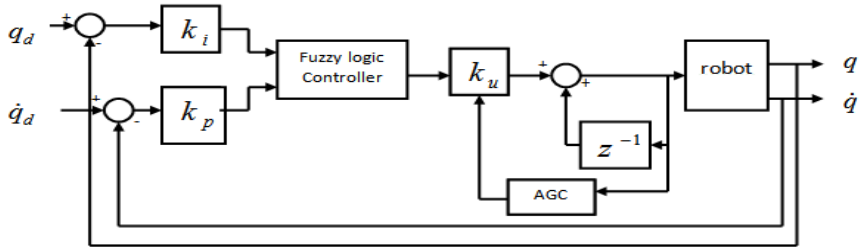

a. The improved fuzzy PI control system

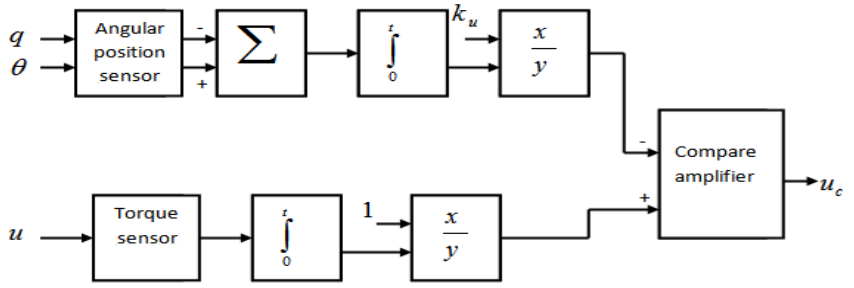

b. The automatic gain control circuit

Fig. 9. The block diagram of MFPIC.

The control performance of the MFPIC is not satisfactory as shown in Fig. 10. The amplitudes of the oscillations for joints 1 and 2 are increasing because of flexibility in the joints. The tracking performance of joint 3 shows high frequency oscillations which is not satisfactory, as well. The maximum values of tracking errors for the joints 1, 2, 3 and 4 are $0.25rad$, $0.23rad$, $0.023m$ and $0.089rad$, respectively. The control efforts are shown in Fig. 11. Joint 3 shows high frequency oscillations. Joint 4 shows a high torque with a maximum value of $615Nm$. Compared with the DAFC, the control performance of the DAFC is much better as shown by simulations.

Table 4. The parameters of controllers for the MFPIC.

Controller	1	2	3	4
k_i	1.5	1.5	0.02	0.04
k_p	0.5	0.25	0.4	0.05

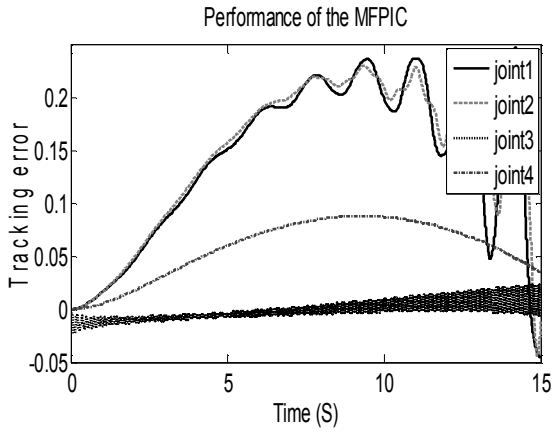

Fig. 10. The performance of the MFPIC

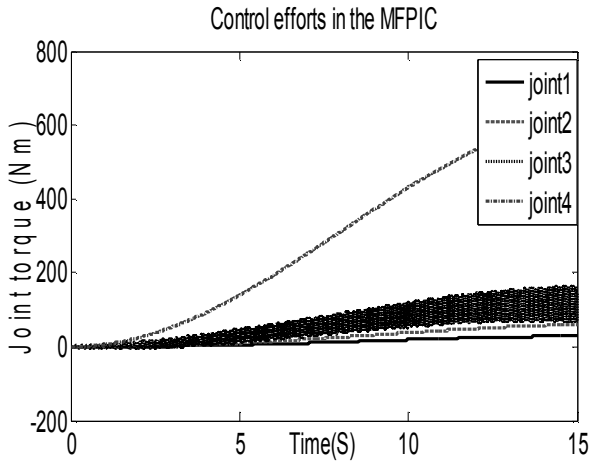

Fig. 11. Control efforts of the MFPIC

5. CONCLUSION

A novel fuzzy controller has been designed for flexible-joint robots based on the Lyapunov stability method. The proposed controller is in the class of decentralized direct adaptive fuzzy controllers. Compared with a torque-based controller, it is more effective by considering the whole robotic system including the robot manipulator and its motors. The fuzzy controller has been able to overcome the complexity of system. The proposed control design has a simpler structure than the common control of flexible-joint robots. It uses only one control loop using the voltage control strategy while others employs two control loops using the torque control strategy. The control method has been verified by stability analysis. The simulation results have shown the superiority of the proposed design over the modified proportional-integral fuzzy controller.

REFERENCES

Brogliato, B., Ortega, R., and Lozano, R. (1995). Global tracking controllers for flexible-joint manipulators: a comparative study. *Automatica*, 31(7), 941–956.

Fateh, M.M. (2008). On the voltage-based control of robot manipulators. *International Journal of Control, Automation, and Systems*, 6(5), 702–712.

Fateh, M.M. (2012a). Robust control of flexible-joint robots using voltage control strategy. *Nonlinear Dynamics*, 67(2), 1525–1537.

Fateh, M.M. (2012b). Nonlinear control of electrical flexible joint robots. *Nonlinear Dynamics*, 67(4), 2549–2559.

Gürkan, E., Erkmen, I., and Erkmen, A.M. (2002). Two-way fuzzy adaptive identification and control of a flexible-joint robot arm. *Information Sciences*, 145(1-2), 13–43.

Homaifar, A., Sayyarrodsari, B., and Hogans, J.E. (1994). Fuzzy controller for robot arm trajectory. *Information Sciences*, 2(2), 69–83.

Hsua, S.H. and Fua, L.C. (2006). A fully adaptive decentralized control of robot manipulators. *Automatica*, 42(10), 1761–1767.

Jabri, D., Guelton, K., Manamanni, N., Jaadari, A. and Chinh, C.D. (2012). Robust stabilization of nonlinear systems based on a switched fuzzy control law. *Journal of Control Engineering and Applied Informatics*, 14(2), 40-49.

Kugi, A., Ott, C., Albu-Schaffer, A., and Hirzinger, G. (2008). On the passivity-based impedance control of flexible joint robots. IEEE Trans. Robotics and Automation, 24(2), 416–429.

Lendek, Zs, Babuska, R. and De Schutter, B. (2010). Stability bounds for fuzzy estimation and control, *Journal of Control Engineering and Applied Informatics*, 12 (3), 3-12.

Li, T.S., Tong, S.C., and Feng, G. (2010). A novel robust adaptive fuzzy tracking control for a class of nonlinear multi-input/multi-output systems. *IEEE Trans. Fuzzy Systems,* 18(1), 150–160.

Li, T.H.S. and Huang, Y.C. (2010). MIMO adaptive fuzzy terminal sliding-mode controller for robotic manipulators. *Information Sciences*, 180(23), 4641–4660.

Liua, C., Cheahb, C.C., and Slotine, J.J.E. (2008). Adaptive task-space regulation of rigid-link flexible-joint robots with uncertain kinematics. *Automatica*, 44, 1806–1814.

Luca, A.D., Isidori, A., and Nicolo, F. (1985). Control of robot arm with elastic joints via nonlinear dynamic feedback. 24th IEEE Conf. on Decision and Control, Ft. Lauderdale, FL, 24, 1671–1679.

Marino, R. and Nicosia, S. (1988). Singular perturbation techniques in the adaptive control of elastic robots. In: Proc IFAC SYCORO'85, Barcelona, Spain, 95-100.

Seraji, H. (1989). Decentralized adaptive control of manipulators: theory, simulation, and experimentation. *IEEE Trans. Robotics and Automation*, 5(2), 183–200.

Spong, M.W., Khorasani, M.W., and Kokotovic, P.V. (1987a). An integral manifold approach to the feedback control of flexible joint robots. *IEEE Trans. Robotics and Automation,* 3(4), 291–300.

Spong, M.W. (1987b). Modeling and control of elastic joint robots. *ASME Trans. Dynamical Systems, Measurement and Contrrol*, 109, 310–319.

Spong, M.W. (1985). Adaptive control of flexible joint manipulators: comments on two papers. *Automatica*, 3, 585–590.

Sweet, L.M. and Good, M.C. (1985). Redefinition of the robot motion control problem. *IEEE Control System Magazine*, 5(3), 18–25

Talole, E., Kolhe, P., and Phadke, B. (2010). Extended State Observer based Control of Flexible Joint System with Experimental Validation. *IEEE Trans. Industrial Electronics*, 57(4), 1411–1419.

Tang, W., Chen, G., and Lu, R. (2001). A modified fuzzy PI controller for a flexible-joint robot arm with uncertainties. *Fuzzy Sets and Systems*, 118, 109–119.

Tomei, P. (1991). A simple PD controller for robots with elastic joints. *IEEE Trans. Automation and Control*, 36(10), 1208–1213.

Tong, S., Li, H.X., and Chen, Li, H.X. (2004). Adaptive fuzzy decentralized control for a class of large-scale nonlinear systems. IEEE Trans. Systems, Man and Cybernetics-Part B, 34(1), 770–775.

Tong, S., Li, H.X., and Wang, H.X. (2004). Observer-based adaptive fuzzy control for SISO nonlinear systems. *Fuzzy Sets and Systems*, 148, 355-376.

Tong, S., Li, Y., and Liu, Y. (2011). Observer-based adaptive fuzzy backstepping control for a class of stochastic nonlinear strict-feedback systems. I*EEE Trans. Systems Man and Cybernetics* -Part B, 41(6), 1693–1704.

Wang, L.X. (1996). *A course in fuzzy systems and control*, Prentice Hall, Englewood Cliffs, NJ.

Wang, L.X. (1994). *Adaptive fuzzy systems and control: design and stability analysis*, Prentice-Hall, Englewood Cliffs, NJ.

Wang, D. (1995). A simple iterative learning controller for manipulators with flexible joints, *Automatica,* 31, 1341–1344.

Wilson, G.A. (1994). Robust tracking of elastic joint manipulators using sliding mode control, *Transactions of the Institute of Measurement and Control,* 16(2), 99–107.

Zeman, V., Patel, R.V., and Khorasani, K. (1997). Control of a flexible-joint robot using neural networks, *IEEE Trans. Control System Technology,* 5(4), 453–462.